Unsteady Propagation of Stick-Slip in a Nonuniform Stress Field

著者	Kato Naoyuki, Lu Zhenye, Kosuga Masahiro, KYamamoto Iyohiko, Hirasawa Tomowo
雑誌名	The science reports of the Tohoku University. Fifth series, Tohoku geophysical journal
巻	33
号	3-4
ページ	263-272
発行年	1990-12
URL	http://hdl.handle.net/10097/45335

Tôhoku Geophys. Journ. (Sci. Rep. Tôhoku Univ., Ser. 5), Vol. 33, Nos. 3, 4, pp. 263-271, 1990

Unsteady Propagation of Slick-Slip in a Nonuniform Stress Field

NAOYUKI KATO[1], ZHENYE LU[2], MASAHIRO KOSUGA[3], KIYOHIKO YAMAMOTO[1] and TOMOWO HIRASAWA[1]

(received August 30, 1990)

Abstract: A stick-slip experiment is carried out in order to clarify the effects of stress nonuniformity on rupture propagation. The simulated fault prepared for the experiment has two hollow holes to produce an extremely nonuniform stress field. The rupture propagation is found to be arrested temporarily or completely at an edge of the holes. This rupture arrest is caused by a high shear strength due to a high concentration of normal stress and by deficiency in the strain energy available in localized regions near the edge.

1. Introduction

From the viewpoint of seismology one of the most interesting subjects in the source process of earthquakes is how earthquake faulting starts and stops, or how the size of earthquake is determined. It is considered that various kinds of nonuniformities such as those in structure, material and stresses play an important part in controlling rupture or slip propagation on faults. The nonuniformities are thus considered to be the key to the arrest mechanism of rupture propagation. Kikuchi and Takeuchi (1971), Husseini *et al.* (1975), Das and Aki (1977), Aki (1979), King (1986), and others have actually suggested some mechanisms of rupture arrest; insufficient strain energy available, high strength barrier, fault bend, *etc*. It should be meaningful to examine experimentally the dynamic behavior of stick-slip propagation on a simulated nonuniform-fault.

Some experimental studies have been made for the effects of nonuniformities on stick-slip propagation using large scale rock samples. Dieterich (1981) performed experiments on a granite sample having a 2 m long pre-cut fault with a large scale biaxial testing machine. He observed unstable slip events whose rupture areas were confined to a part of the entire fault. He concluded for the confined slip events that the minimum dimension of slipped area depended both on the roughness of the sliding surfaces and on the normal stress applied to the fault. Using the same loading apparatus that Dieterich (1981) did, Lockner *et al.* (1982) generated confined stick-slip events by means of selectively varying pore pressures or effective normal stresses. High pore pressures were introduced in the two fault-end regions so that free sliding might occur

[1] Observation Center for Prediction of Earthquakes and Volcanic Eruptions, Faculty of Science, Tôhoku University, Sendai 980

[2] Center for Analysis and Prediction, State Seismological Bureau, Beijing, People's Republic of China

[3] Earthquake and Volcano Observatory, Faculty of Science, Hirosaki University, Hirosaki 036

prior to the occurrence of a stick-slip event. Even when the central locked region of the fault slipped and a stick-slip event occurred, the slip did not propagate through the fault-end regions where shear strain had not been sufficiently accumulated.

Kuwahara (1985), Ohnaka *et al.* (1986), and Kato *et al.* (1989) have carried out stick-slip experiments using rock samples with about 40 cm long simulated faults to examine the effects of nonuniformities of sliding surfaces and/or local stresses on the dynamic behavior of stick-slip. Kuwahara (1985) observed the arrest of stick-slip propagation for the first and, sometimes, for the second event in a series of slip events generated repeatedly. He attributed the rupture arrest to the nonuniformity of local stress fields, which was decreased with an increase in the event number. Kato *et al.* (1989) prepared a granite sample whose sliding surfaces were artificially undulated so that the local normal stress and, consequently, the local shear strength became nonuniform along the fault. They found that stick-slip events stopped propagating at high normal stress regions or high strength barriers.

In contrast to the high strength barrier, we may expect that a weak region of a fault prevents the shear stress from concentrating strongly at the vicinity of a crack tip not to provide a sufficient amount of strain energy necessary for further advance of rupturing. The region can be regarded as a barrier to dynamic rupturing, though its stress state is contrary to that of the high strength barrier. This may be similar to high pore pressure regions in the experiments by Lockner *et al.* (1982). In the present study we prepare a rock sample with hollow holes in a pre-existing fault. The holes, of course, have no strength and no stresses, and can be considered as an extreme case of materials of small elastic constants.

2. Experiment

2.1. Method

The detailed description of our experimental procedure have already been given in Kato *et al.* (1989). We recapitulate it and describe rather in detail the rock sample

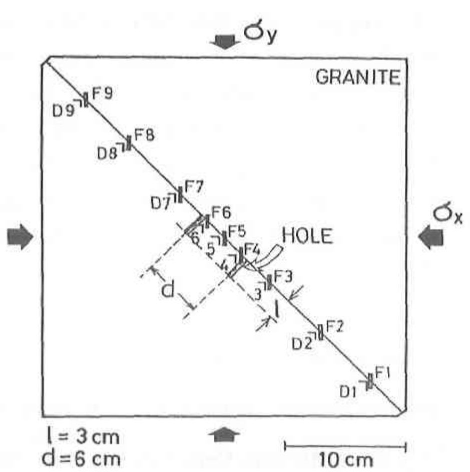

Fig. 1 Schematic diagram of rock sample with two rectangular hollow holes in a pre-existing fault. The symbols D1 to D9 stand for shear strain sensors and F1 to F9 stand for relative displacement sensors. The symbols l and d denote the hole depth and the distance between the center lines of the two holes, respectively.

specially designed for the present study. The rock sample, 30 cm × 30 cm × 10 cm in size, was biaxially pressed at a constant shear strain rate of 10^{-6}/s with a loading apparatus to generate stick-slip events on a pre-existing fault of about 40 cm in length. The rock sample was made of Higashiyama granite, whose P- and S- wave speeds are 5.5 km/s and 3.3 km/s, respectively.

Figure 1 shows the sample configuration. Two rectangular holes (notches), whose depths and widths are 3 cm or 7 cm and 1 cm, are bored in a fault surface. The distance between the center lines of the two notches are 6 cm along the fault strike. The sliding surfaces of the granite sample were carefully ground with abrasive to have a sufficiently small waviness. We measured the topography of the two sliding surfaces with a stylus profilometer. We obtained the cutoff wavelength of about 10 μm for the power spectra of the surface traces. According to Kuwahara (1985), stick-slip is easy to occur on the sliding surfaces of this degree of the surface roughness in the case of granite sample.

The relative displacements across the fault and the shear strains near the fault were measured with stɪain gauge sensors. The sensors were aligned along the fault as shown in Fig. 1. The dynamic strain signals were amplified and digitized with a resolution of 8 or 10 bits at a sampling frequency of 500 kHz or 1 MHz. This recording system had to be triggered because of limited memory length of 2048 words per channel. Since an acoustic emission event was expected to accompany a stick-slip event, the acoustic emission detected with a piezoelectric transducer was used as a trigger source. In addition to the sensors for dynamic strain measurements, we pasted strain gauge sensors along the fault to monitor the quasi-static fields of shear strain near the fault. These signals were continuously digitized at a sampling frequency of about 6Hz and stored in a mini-computer system.

2.2. Results

Figure 2 shows examples of the time histories of relative displacements and shear stresses observed for a stick-slip event. The event was generated on the fault with the notch depth of 3 cm at an average normal stress of 5.0 MPa. The time of sharp onset in relative displacement was taken as the rupture time at each sensor position. The observed rupture times are plotted in Fig. 3 as a function of distance along the fault. The data designated as A in the figure were obtained for the stick-slip event shown in Fig. 2. It is noted that the two notches were located between sensors 3 and 4, and between sensors 6 and 7, respectively. The rupture of event A, which had been initiated at some point near sensor 7, propagated rather unilaterally toward the position of sensor 8, as seen in Fig. 3. We have no information whether the rupture propagated also toward sensor 6 at a small speed or the rupture was initiated again at some point near sensor 6. However, if we assume that the rupture propagated from sensor 7 to sensor 6, the apparent rupture velocity V_R between the two sensors is calculated to be about 400 m/s. The apparent rupture velocity in the other notch region between sensors 4 and 3 is about 800 m/s. These values are much lower than the rupture velocities (greater than 2 km/s) observed in fault regions without notches. We confirmed that most of the slip

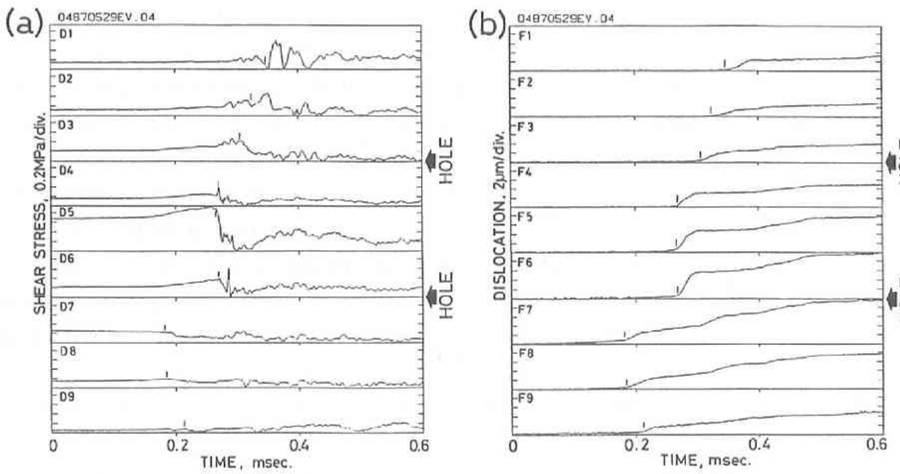

Fig. 2 Examples of (a) shear stress and (b) relative displacement records obtained for a stick-slip event on the fault with two holes. The hole depth and the average normal stress are 3 cm and 5.0 MPa, respectively. The tick marks in (b) indicate the times of sharp onset in relative displacements. They are given also in (a) for the sake of reference.

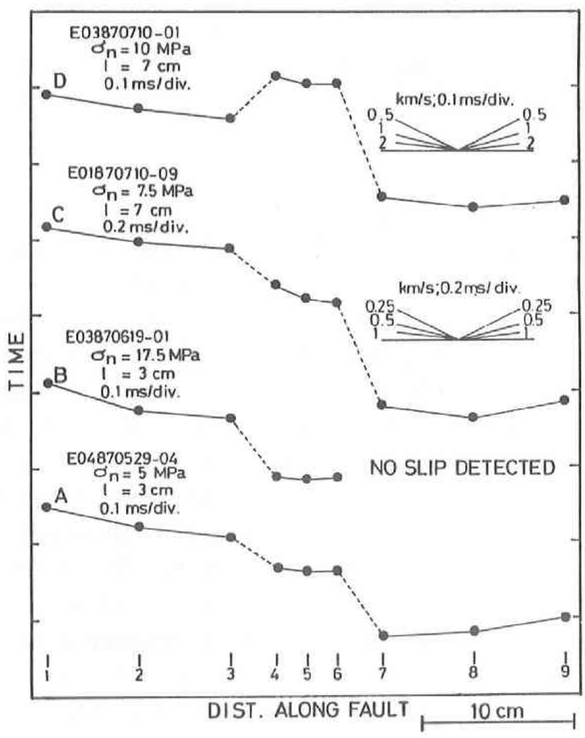

Fig. 3 Space-time views of rupture propagation for stick-slip events on the fault with two holes. The average normal stress σ_n and the hole depth l are given in the figure.

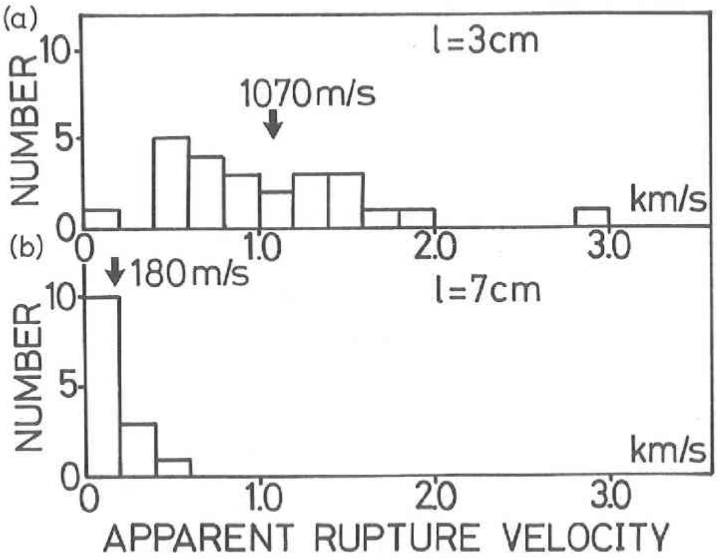

Fig. 4 Histograms for the observed apparent rupture velocity V_R between sensors 3 and 4, and between sensors 6 and 7 at an average normal stress of 7.5 MPa. (a) The case of 3 cm in hole depth. (b) The case of 7 cm in hole depth. The average value of V_R for each case is indicated by an arrow in the figure.

events showed a similar time delay in rupture propagation at the vicinities of the holes. In some few cases we observed the complete arrest of rupture propagation near a hole. The holes on the fault are thus found to act as barriers.

Figure 4 shows histograms for the observed apparent rupture velocity V_R between two sensors which sandwich a hole (*i.e.*, sensors 3 and 4, or sensors 6 and 7). The data were obtained at an average normal stress of 7.5 MPa in the cases of two notch depths; (a) is for $l=3$ cm and (b) is for $l=7$ cm. In the latter case of notch depth, we found two events in which the rupture stopped propagating near a hole and did not start again. These two special cases of the complete arrest are included in the number of stick-slip events having V_R in the range between 0 km/s and 0.2 km/s. These histograms together with the mean values of the apparent rupture velocities clearly indicate that the local values of V_R near holes are abnormally small in comparison with the values of 2 to 3 km/s observed in the other fault regions. It is also clear from the figure that the values of V_R are distinctly smaller in the case of $l=7$ cm than those in the case of 3 cm. It is noted that the same tendency was observed also for other cases of average normal stresses, though the results are omitted here.

3. Discussion

3.1. Effect of Static Stress Field

Let us consider the case that a rock specimen as used in the present experiment is biaxially compressed to be under an elastically equilibrium state. It is reasonable to

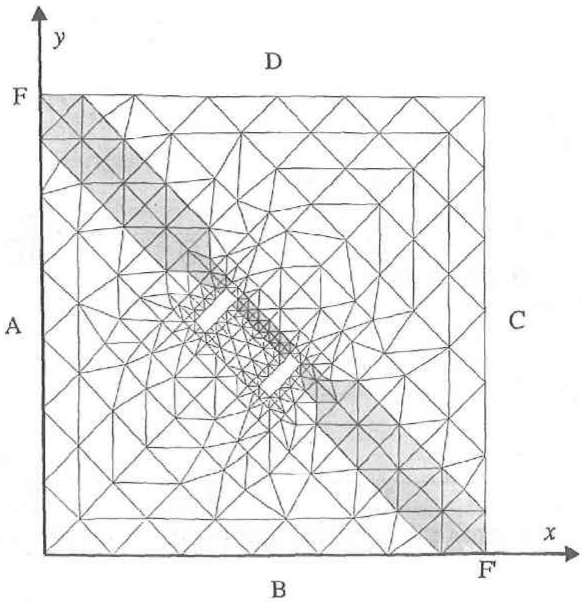

Fig. 5 Grids and coordinates used in the finite element calculation of two-dimensional stress field in the rock sample with two rectangular holes of 3 cm depths. The calculated results for shaded elements along the simulated fault F-F′ are given in Figs. 6 and 7. Symbols A, B, C, and D represent sample sides where boundary conditions are given (see text).

expect for the specimen that not only the shear stress but also the normal stress concentrate in the vicinities of the notch edges on the fault. This normal stress concentration may enhance the shear strength of the fault. Kosuga and Anami (1989) and Anami and Kosuga (1990) have made numerical simulations for the stress field produced in a biaxially compressed rock sample whose configuration is the same as ours. They compared the shear strain field computed by means of a finite element method with that we measured, and found that the comparison is generally satisfactory with some exceptions. We recalculate the stress field in the rock sample by the same method as Kosuga and Anami (1989) with finer grid intervals to examine in a greater detail the stress field near the holes. The finite element grids and coordinates are shown in Fig. 5. We treat the problem as a two dimensional one and assume the condition of plane stress in the calculation. This is because the sample thickness of 10 cm is shorter than the fault length of 40 cm, and, besides, the calculated results can be compared only with the measured strains on the free surfaces of the sample. It has been shown by Kosuga and Anami (1989) that the stresses calculated by a plane stress finite element method is very similar to those on a free surface calculated by a three dimensional method. The boundary conditions on sides A to D in Fig. 5 are assumed as follows;

$u=0,\ \sigma_{xy}=0$ on side A,

$v=0,\ \sigma_{xy}=0$ on side B,

$\sigma_{xx}=7.5$ MPa, $\sigma_{xy}=0$ on side C,
$\sigma_{yy}=2.5$ MPa, $\sigma_{xy}=0$ on side D,

where σ_{ij} is the stress tensor and u and v are displacements in the x and y directions, respectively.

The calculated stress field in the sample is close in general to the results given by Kosuga and Anami (1989), and hence we present here only the results of particular interest for stresses along the fault (F–F′ in Fig. 5). Figure 6 shows the ratio of the shear stress to the normal stress applied to the fault, and Fig. 7 the strain energy density in shaded elements along the fault (Fig. 5). The figures show that these quantities are distributed anti-symmetrically about the holes. The results in Figs. 6 and 7 indicate that the rupture may be arrested at left sides of the holes in the figures. However, we have no information whether the rupture stops at the left side or the right side of a hole, because the resolution of our measurement is limited by the sensor interval of a few cm (Fig. 1). The effect of the holes of 7 cm depths on the rupture deceleration is more significant than that of 3 cm depths as found in Fig. 4. Kosuga and Anami (1989) have stated that the stress nonuniformity around the holes of 7 cm depths is larger than that of 3 cm depths. This and our results indicate that the stress nonuniformity around holes plays an important part in the rupture arrest.

3.2. *Effects of the Dynamic Loading*

In addition to the effect of the stress field in a static equilibrium, the effect of dynamic stress field is important on the rupture propagation. When rupture is propagating, the shear stress is concentrated dynamically in a region near the rupture front to accelerate or to maintain the rupture velocity. This is the general situation of propagating rupture. In the present case in which rupture approaches an edge of a notch, however, a sufficient amount of shear stress concentration is not expected in the notch

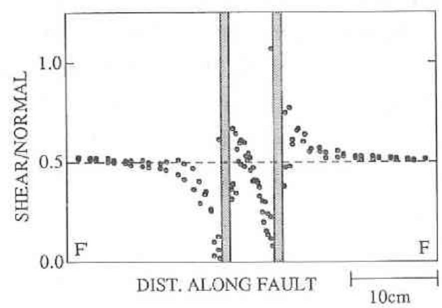

Fig. 6 Calculated ratio of shear stress to normal stress applied to the fault in elements along the fault F–F′ in Fig. 5. The average value of the ratio, 0.5, is shown by the dotted line. Shaded areas show the locations of holes.

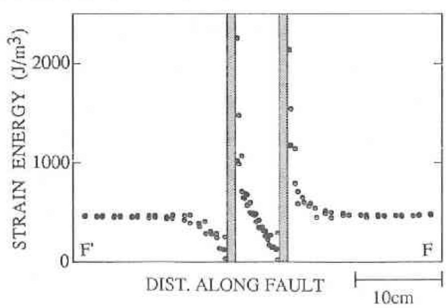

Fig. 7 Calculated strain energy density stored in elements along the fault F–F′ in Fig. 5. Shaded areas show the locations of holes.

region. In other words, the strain energy available is insufficient for breaking the contact of fault surfaces near the other edge of the notch. It is suggested that this deficiency in strain energy or in shear stress concentration causes the halt or the arrest of rupture propagation.

As seen in the examples of Figs. 2 and 3, most of the rupture events that had stopped near a hole started to propagate again. The mean values of the time interval for events at an average normal stress of 7.5 MPa (Fig. 4) are 40 μs for $l=3$ cm and 304 μs for $l=7$ cm. In calculating the mean time interval we excluded the results of two events for $l=7$ cm where rupture stopped completely. Since this time interval is too short for the ram of our loading apparatus to make a significant increase in the applied stress, the rupture is considered to start again spontaneously. Stress concentration at the opposite edge of the notch due to Rayleigh waves, which travel along the inner surface of the notch, may contribute to the delayed rupture. Assuming 2.8 km/s for Rayleigh wave velocity, we obtain the travel time of 54 μs for $l=7$ cm and of 25 μs for $l=3$ cm. The time interval of rupture halt is considerably longer than these travel times. This result suggests that the delayed rupture in the region near the notch edge is explained by the delayed stress concentration due to Rayleigh waves in cooperation with the time-dependent property of shear strength (*e.g.*, Das and Scholz, 1981).

4. Conclusion

We found from the present stick-slip experiment that the propagation of shear rupture is arrested temporarily or completely near a hollow hole along the fault. This rupture arrest is caused by cooperation of a high shear strength due to a high concentration of normal stress with deficiency of the strain energy available in the vicinity of a hole edge. Although no large hollow holes exist along active faults in the real earth, the regions of small effective elastic constants are considered to play a similar role in controlling the dynamic behavior of rupture propagation.

Acknowledgments : We are grateful to Dr. Y. Kuwahara of Geological Survey of Japan and Prof. M. Ohnaka of Earthquake Research Institute, University of Tokyo, for their valuable discussion. We are indebted to Prof. A. Takagi, Prof. H. Hamaguchi, and Prof. A. Hasegawa for their helpful comments. We thank Dr. S. Horiuchi for his critically reviewing the manuscript and making valuable comments. This study was partly supported by a grant-in-aid for co-operative research from the Ministry of Education, Science and Culture of Japan (Project Number 61302022).

References

Aki, K., 1979 : Characterization of barriers on an earthquake fault, *J. Geophys. Res.*, **84**, 6140-6148.

Anami, T. and M. Kosuga, 1990 : Stress field analysis in the rock specimen during stick-slip experiment by finite element method, *Quart. J. Seism.*, **53**, 23-29 (in Japanese with English abstract).

Das, S. and K. Aki, 1977 : Fault plane with barriers : A versatile earthquake model, *J. Geophys. Res.*, **82**, 5658-5670.

Das, S. and C.H. Scholz, 1981: Theory of time dependent rupture in the earth, *J. Geophys. Res.*, **86**, 6039-6051.

Dieterich, J.H., 1981: Potential for geophysical experiments in large scale tests, *Geophys. Res. Lett.*, 8, 653-656.

Husseini, M.I., D.B. Jovanovich, M.J. Randall and L.B. Freund, 1975: The fracture energy of earthquakes, *Geophys. J.R. astr. Soc.*, **43**, 367-385.

Kato, N., Y. Kuwahara, K. Yamamoto and T. Hirasawa, 1989: An experimental study of the dynamic behavior of stick-slip on a nonuniform strength fault, *Tôhoku Geophys. J.* (*Sci. Rep. Tôhoku Univ., Ser. 5*), **32**, 1-20.

Kikuchi, M. and H. Takeuchi, 1972: Stop mechanism of crack propagation, *Zisin, Ser. 2*, **24**, 298-303 (in Japanese with English abstract).

King, G.C.P., 1986: Speculations on the geometry of the initiation and termination processes of earthquake rupture and its relation to morphology and geological structure, *Pure Appl. Geophys.*, **124**, 567-585.

Kosuga, M. and T. Anami, 1989: Stress field in a rock specimen during stick-slip. (1) Finite element analysis of a sticking stage, *Sci. Rep. Hirosaki Univ.*, **36**, 92-101 (in Japanese with English abstract).

Kuwahara, Y., 1985: An experimental study on dynamic sliding process during stick-slip and its implication to earthquake faulting, Ph. D. Thesis, Tohoku University, 130 pp.

Lockner, D.A., P.G. Okubo and J.H. Dieterich, 1982: Containment of stick-slip failures on a simulated fault by a pore injection, *Geophys. Res. Lett.*, **9**, 801-804.

Ohnaka, M., Y. Kuwahara, K. Yamamoto and T. Hirasawa, 1986: Dynamic breakdown processes and the generating mechanism for high-frequency elastic radiation during stick-slip instabilities, in *Earthquake Source Mechanics* (edited by S. Das, J. Boatwright, and C.H. Scholz), *A.G.U. Maurice Ewing Ser.*, **6**, 13-24.